PROCEEDINGS OF SCIENCE

CP violation in *B* hadron decays

Mark Whitehead[a,*]

[a] *University of Bristol,*
H.H. Wills Physics Laboratory, Bristol, United Kingdom

E-mail: mwhitehe@cern.ch

The experimental status of charge-parity (*CP*) violation measurements in the decays of *B* hadrons is reviewed. The latest results from the LHC experiments are presented, including measurements of the CKM parameters γ and ϕ_s, a search for *CP* violation in baryonic decays and a study of the $B^+ \to \pi^+\pi^+\pi^-$ channel.

The Eighth Annual Conference on Large Hadron Collider Physics-LHCP2020
25-30 May, 2020
online

*Speaker

PoS(LHCP2020)190

1. Introduction

A complete explanation of the matter-antimatter asymmetry of the Universe remains a mystery. One ingredient, known as charge-parity (*CP*) violation, allows the decays of particles and antiparticles to be different. The standard model (SM) of particle physics includes *CP* violation, but the known sources can only explain a minuscule fraction of the observed universal asymmetry. This implies that there must be further sources of *CP* violation that are not included in the current theory. These sources may be from new interactions or new particles, generically know as new physics (NP). Studies of *CP* violation therefore provide a precise test of the SM and the potential to observe NP effects beyond it.

2. Unitarity triangles

The Cabibbo-Kobayashi-Maskawa (CKM) matrix describes the quark-level transitions of the weak interaction. Unitary constraints can be used to define unitarity triangles, each with an area proportional to the total amount of *CP* violation in the quark sector. Measurements of the angles and sides of these triangles provide strict tests of the SM and the assumption of unitarity.

2.1 Measurements of γ

Measurements of the angle γ, defined as $\gamma = \arg\left(-\frac{V_{ud}V_{ub}^*}{V_{cd}V_{cb}^*}\right)$, provide a standard candle test of the SM because it can be measured purely from tree-level decay processes. These are expected have smaller (but non-zero [1]) corrections from possible NP effects compared to loop-level topologies. Global fits to the CKM parameters can also infer the value of γ indirectly, a precise comparison of the direct and indirect approaches is crucial. The current world average of direct γ measurements is $\gamma = \left(71.1^{+4.6}_{-5.3}\right)^\circ$ [2] and the indirect values are $\gamma = \left(65.7^{+0.9}_{-2.7}\right)^\circ$ [3] and $\gamma = (65.8 \pm 2.2)^\circ$ [4]. The LHCb measurement of γ using $B^0 \to DK^{*0}$ decays, where D is an admixture of D^0 and $\bar{D}^0$ mesons, is described in detail in Ref. [5]. The analysis is based on a 4.8 fb^{-1} data sample collected between 2011 and 2016. The D mesons are reconstructed in the $K^\pm\pi^\mp$, K^+K^-, $\pi^+\pi^-$, $K^\pm\pi^\mp\pi^\pm\pi^\mp$ and $\pi^+\pi^-\pi^+\pi^-$ final states. Fits are performed to the B^0 and (right) $\bar{B}^0$ candidates, tagged by the charge of the kaon from the $K^{*0} \to K^-\pi^+$ decay, to measure the yields for each sample. An example is shown for the first observation of the $D \to \pi^+\pi^-\pi^+\pi^-$ sub-channel in Fig. 1 (left). The yields are used to calculate a set of asymmetries and yield ratios that are sensitive to γ [5]. Combining these for each of the D final states gives the constraints shown in Fig. 1 (right). These are the most precise results from B^0 mesons and will be added to future experimental combinations.

2.2 Measurements of ϕ_s

The angle ϕ_s is the mixing phase in the process of B_s^0-$\bar{B}_s^0$ oscillations. It is defined as $\phi_s \approx -2\beta_s = -2\arg\left(-\frac{V_{ts}V_{tb}^*}{V_{cs}V_{cb}^*}\right)$, and is measured to be $\phi_s = -0.021 \pm 0.031$ rad [2] (prior to the new results below). Using CKM unitarity, the expected values are $\phi_s = \left(-0.0369^{+0.0010}_{-0.0007}\right)$ rad [3] and $\phi_s = (-0.0370 \pm 0.0010)$ rad [4]. However, this SM value can be significantly modified by contributions from NP processes so a precise experimental value is critical to make a meaningful comparison with expectation. New results from LHCb [6], ATLAS [7] and CMS [8] are below.

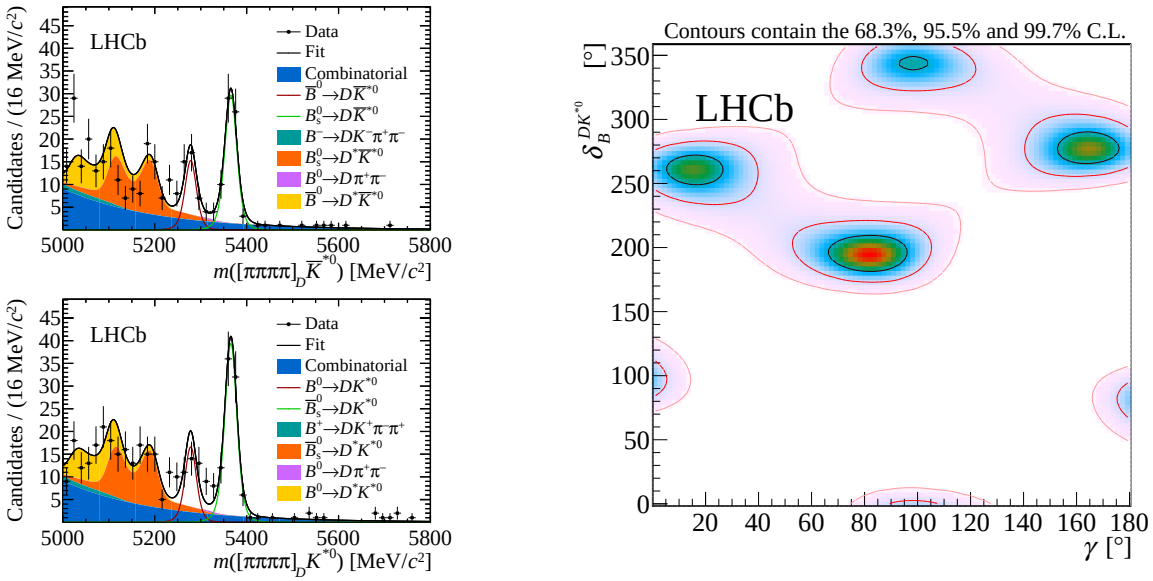

Figure 1: Fit to the B candidate invariant mass distribution for (top left) $\bar{B}^0$ and (bottom left) B^0 candidates. (Right) constraints on γ and the strong-phase. Reproduced from Ref. [5].

LHCb

This measurement uses data from 2015 and 2016 to analyse $B^0_s \to J/\psi K^+K^-$ decays, with $J/\psi \to \mu^+\mu^-$ and $m(K^+K^-)$ in a 60 MeV window around the ϕ meson. The result is obtained from a time-dependent angular analysis performed simultaneously in six bins of $m(K^+K^-)$. Projections of the fit are compared to the data in Fig. 2 (left) for the B candidate invariant mass and decay time distributions. There are around 120000 signal events with a flavour tagging power of about 4.7%. The fit determines $\phi_s = (-0.083 \pm 0.041 \pm 0.006)$ rad where the first uncertainty is statistical and the second systematic. This is combined with the result from Run 1 to give $\phi_s = (-0.081 \pm 0.032)$ rad where the uncertainties are combined. Finally, all of the LHCb measurements are combined to give $\phi_s = (-0.042 \pm 0.025)$ rad, as shown in Fig. 2 (right).

ATLAS

This analysis of $B^0_s \to J/\psi\phi$ decays is based on a sample of 80.5 fb^{-1} recorded during LHC Run 2. A multi-dimensional fit including the B candidate mass, proper decay time and uncertainty, and decay angles is performed. Projections of the fit are shown in Fig. 3 for the invariant mass distributions (left) and proper decay time (centre). A large signal yield in excess of 450000 candidates is found, with flavour tagging power at around 1.75%. The result, including a combination with Run 1 as shown in Fig. 3 (right), of $\phi_s = (-0.087 \pm 0.036 \pm 0.017)$ rad is both consistent and competitive with the LHCb measurement. Here the first uncertainty is statistical and the second systematic. The larger signal yield and lower flavour tagging power larger cancel out to give a similar statistical uncertainty.

CMS

This analysis uses data from 2017 and 2018 to measure ϕ_s using $B^0_s \to J/\psi\phi$ decays. The selection strategy is different to that of ATLAS, focusing on high flavour tagging power rather than high

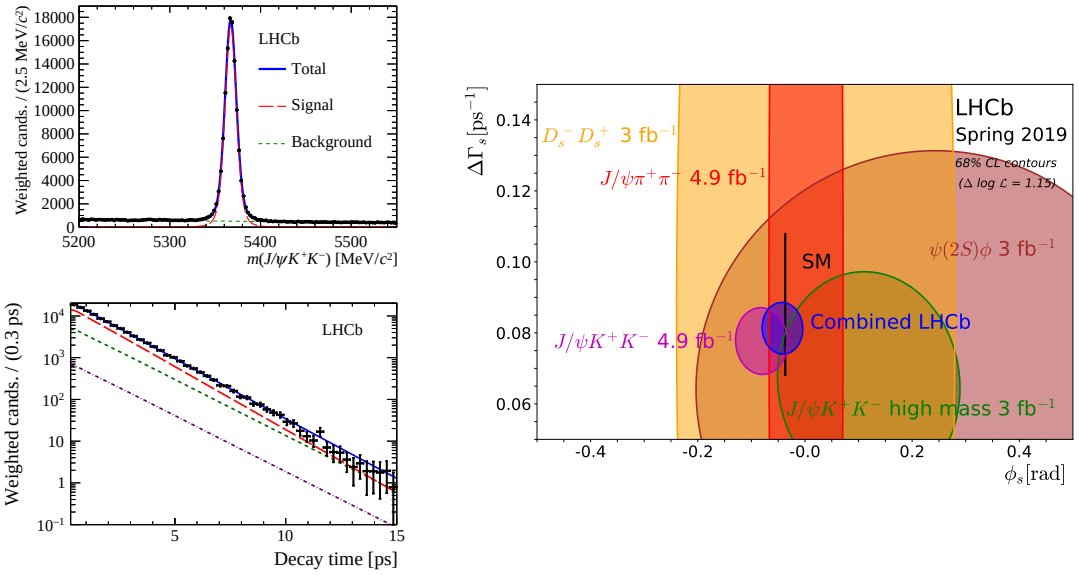

Figure 2: Projections of the fit for the B candidate mass (top left) and proper decay time (bottom left) distributions. (Right) a combination of LHCb ϕ_s results. Reproduced from Ref. [6].

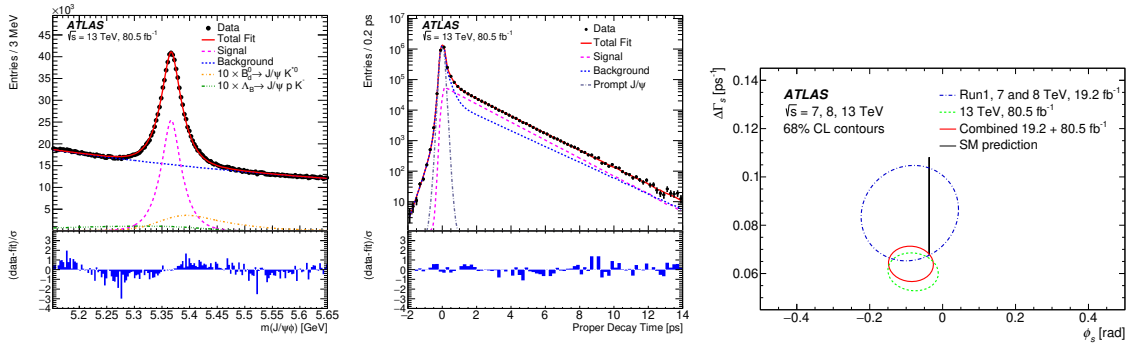

Figure 3: Projections of the fit for the B candidate mass (left) and proper decay time (centre) distributions. (Right) a combination of Run 1 and Run 2 ATLAS results. Reproduced from Ref. [7].

signal efficiency. The fitting strategy is similar to both LHCb and ATLAS, with projections in reconstructed mass (left) and proper decay time (centre) shown in Fig. 4, and gives a signal yield of approximately 50000 candidates. The flavour tagging power is around 10%, which compensates for the lower yield, resulting in a value of $\phi_s = (-0.011 \pm 0.050 \pm 0.010)$ rad where the first uncertainty is statistical and the second systematic. This is competitive and compatible with the measurements from ATLAS and LHCb. A combination with the Run 1 CMS result is shown in Fig 4 (right) and yields $\phi_s = (-0.021 \pm 0.045)$ rad.

2.3 Measurements related to β

The CKM angle β is the mixing phase in B^0-$\bar{B}^0$ meson oscillations, and is defined as $\beta = \arg\left(-\frac{V_{cd}V_{cb}^*}{V_{td}V_{tb}^*}\right)$. A measurement of time-dependent CP violation in $B^0 \to D^{*\pm}D^{\mp}$ decays is described in Ref. [9]. This analysis used the full LHCb data set of 9 fb^{-1}. The following

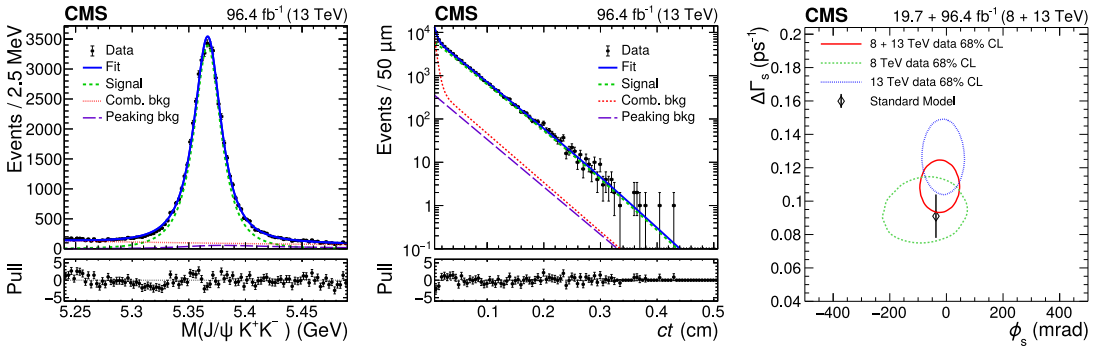

Figure 4: Projections of the fit for the B candidate mass (left) and proper decay time (centre) distributions. (Right) a combination of Run 1 and Run 2 CMS results. Reproduced from Ref. [8].

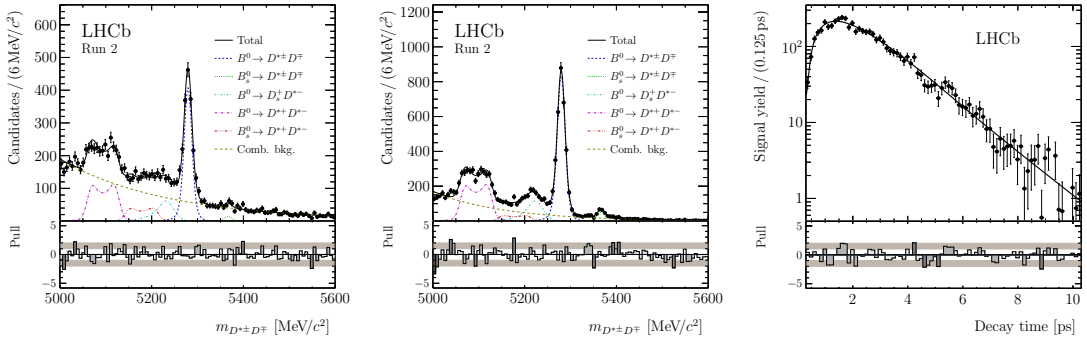

Figure 5: Fit projections for the B candidate invariant mass for the (left) $D^0 \to K^-\pi^+\pi^-\pi^+$ and (centre) $D^0 \to K^-\pi^+$ sub-samples. (Right) a fit to the proper decay time distribution. Reproduced from Ref. [9].

decays are used; $D^{*+} \to D^0\pi^+$, $D^0 \to K^-\pi^+$, $K^-\pi^+\pi^-\pi^+$ and $D^+ \to K^-\pi^+\pi^+$. Firstly, a mass fit is performed to extract weights [10] to statistically subtract background contributions in a subsequent fit to the decay time. Example mass fits for the Run 2 data sample are shown in Fig. 5 for $D^0 \to K^-\pi^+\pi^-\pi^+$ (left) and $D^0 \to K^-\pi^+$ (centre). Four time-dependent decays rates are studied for each combination of B^0 or $\bar{B}^0$ decaying to final state f ($D^{*+}D^-$) or $\bar{f}$ ($D^{*-}D^+$), such as

$$\frac{\mathrm{d}\Gamma_{\bar{B}^0,f}(t)}{\mathrm{d}t} = \frac{e^{-t/\tau_d}}{8\tau_d}(1+\mathcal{A}_{f\bar{f}})\left[1+S_f\sin(\Delta m_d t) - C_f\cos(\Delta m_d t)\right].$$

Where τ_d is the B^0 lifetime, S_f ($S_{\bar{f}}$), C_f ($C_{\bar{f}}$), and $\mathcal{A}_{f\bar{f}}$ are coefficients to be determined and Δm_d is the mass difference between the B^0 mass eigenstates. A background subtracted fit to the proper decay time is performed, as seen in Fig. 5 (right). The observables are then defined and measured to be

$$\begin{aligned}
S_{D^*D} = 0.5(S_f + S_{\bar{f}}) &= -0.861 \pm 0.077 \pm 0.019,\\
\Delta S_{D^*D} = 0.5(S_f - S_{\bar{f}}) &= 0.019 \pm 0.075 \pm 0.012,\\
C_{D^*D} = 0.5(C_f + C_{\bar{f}}) &= -0.059 \pm 0.092 \pm 0.020,\\
\Delta C_{D^*D} = 0.5(C_f - C_{\bar{f}}) &= -0.031 \pm 0.092 \pm 0.016,\\
\mathcal{A}_{D^*D} = \mathcal{A}_{f\bar{f}} &= 0.008 \pm 0.014 \pm 0.006,
\end{aligned}$$

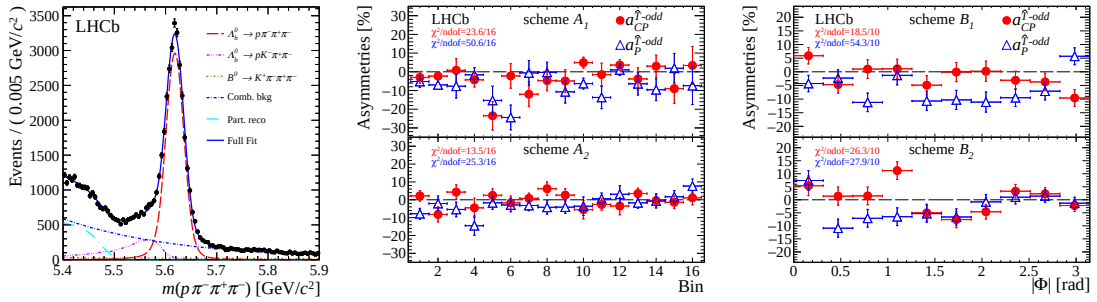

Figure 6: (Left) result of a fit the the reconstructed B candidate mass distribution. (Centre and right) CP (red) and P (blue) asymmetries in bins of the decay phase space. Reproduced from Ref. [12].

where the first uncertainty is statistical and the second systematic. These are the most precise measurements of CP violation in this decay, and exclude CP conservation at the level of 10 σ. No interpretation in terms of β is performed due to the different decay topologies contributing to this decay mode that bring possible NP effects.

3. Baryon CP violation

No CP violation has yet been observed in the baryon sector, although evidence was reported in the $\Lambda_b^0 \to p\pi^-\pi^+\pi^-$ channel using LHCb Run 1 data [11]. An update from LHCb using data from 2011 to 2017 (6.6 fb^{-1}) is described in detail in Ref. [12]. The analysis searches for CP and P violation using triple-product asymmetries and energy test methods. The analysis uses 27600 signal candidates, determined from a fit to the B candidate invariant mass distribution shown in Fig. 6 (left). The results from the triple product asymmetry analysis are shown in Fig. 6 (centre) and (right) for different binning schemes of the decay phase space. The P asymmetries (blue points) are seen to deviate from 0, while those for CP asymmetries (red points) do not. Summing across the bins, P violation is observed at the 5.5 σ level and no evidence for CP violation is seen. Results from the energy test method are in good agreement.

4. CP violation in charmless B decays

Large CP asymmetries were observed by LHCb over the decay phase space of the $B^+ \to \pi^+\pi^+\pi^-$ channel in 2014 [13]. The origin of these effects is studied using an amplitude analysis of 20000 signal candidates from the LHCb Run 1 data sample [14, 15]. A major challenge is to model the $\pi^+\pi^-$ S-wave contribution, three options are used and compared; an isobar model, a K-Matrix term and a quasi-model-independent (QMI) approach. The amplitude squared of these are shown in Fig. 7, where CP violation is seen for the first time and each shows similar behaviour.

A summary of the CP violation effects for each amplitude is given in Table 1, good agreement is seen across the three S-wave scenarios. Significant CP violation is seen in the resonant contributions, in particular for the $f_2(1270)$ state. For the $\rho(770)^0$ resonance, no CP violation is seen in total. However, looking at the CP asymmetry in two mass bins above and below its nominal mass (Fig. 8) shows large, equal and opposite, CP asymmetries that cancel out when integrating over the

amplitude. These results help to understand the origin of the asymmetries observed in the previous analysis, with the first indication of *CP* violation induced by the interference between S and P waves.

5. Summary

The latest results of *CP* violation in *B* hadron decays are presented. These include results to constrain the parameters of the unitarity triangles and searches for *CP* violation in baryonic decays. In the coming years, large data samples from LHC Run 3 and the Belle II experiment will provide more precise results than ever before.

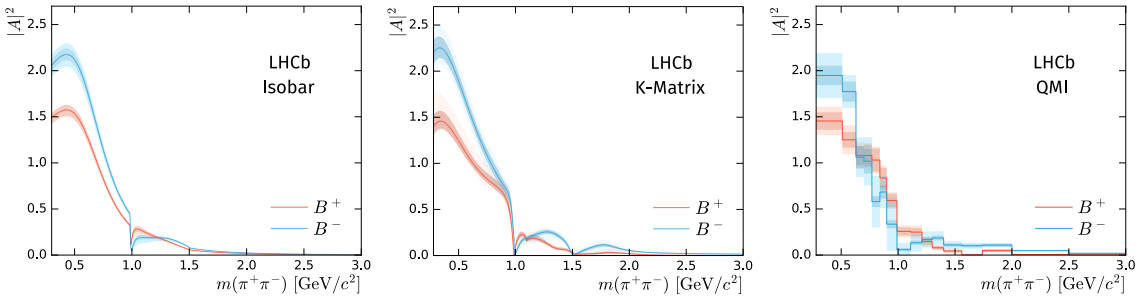

Figure 7: Amplitude squared projections of the three parameterisations of the $\pi^+\pi^-$ S-wave. Reproduced from Ref. [15].

Table 1: *CP* asymmetries for different components of the amplitude models; the uncertainties are statistical, systematic and model related, respectively. Reproduced from Ref. [15].

Component	Isobar	K-matrix	QMI
$\rho(770)^0$	$+0.7 \pm 1.1 \pm 0.6 \pm 1.5$	$+4.2 \pm 1.5 \pm 2.6 \pm 5.8$	$+4.4 \pm 1.7 \pm 2.3 \pm 1.6$
$\omega(782)$	$-4.8 \pm 6.5 \pm 1.3 \pm 3.5$	$-6.2 \pm 8.4 \pm 5.6 \pm 8.1$	$-7.9 \pm 16.5 \pm 14.2 \pm 7.0$
$f_2(1270)$	$+46.8 \pm 6.1 \pm 1.5 \pm 4.4$	$+42.8 \pm 4.1 \pm 2.1 \pm 8.9$	$+37.6 \pm 4.4 \pm 6.0 \pm 5.2$
$\rho(1450)^0$	$-12.9 \pm 3.3 \pm 3.6 \pm 35.7$	$+9.0 \pm 6.0 \pm 10.8 \pm 45.7$	$-15.5 \pm 7.3 \pm 14.3 \pm 32.2$
$\rho_3(1690)^0$	$-80.1 \pm 11.4 \pm 7.8 \pm 24.1$	$-35.7 \pm 10.8 \pm 8.5 \pm 35.9$	$-93.2 \pm 6.8 \pm 8.0 \pm 38.1$
S-wave	$+14.4 \pm 1.8 \pm 1.0 \pm 1.9$	$+15.8 \pm 2.6 \pm 2.1 \pm 6.9$	$+15.0 \pm 2.7 \pm 4.2 \pm 7.0$

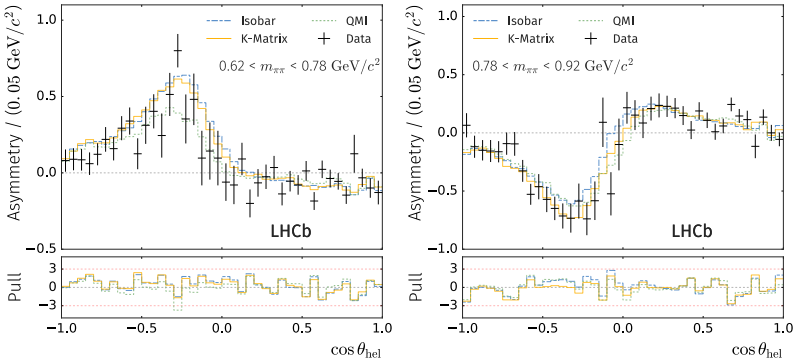

Figure 8: Projections of the amplitude fit in two bins around the $\rho(770)^0$ meson mass, showing the *CP* asymmetry as a function of the helicity angle. Reproduced from Ref. [15].

References

[1] J. Brod, A. Lenz, G. Tetlalmatzi-Xolocotzi and M. Wiebusch, New physics effects in tree-level decays and the precision in the determination of the quark mixing angle γ, Phys. Rev. D **92** (2015) no.3, 033002 [arXiv:1412.1446 [hep-ph]].

[2] HFLAV Collaboration, Y. S. Amhis *et al.*, Averages of b-hadron, c-hadron, and τ-lepton properties as of 2018, [arXiv:1909.12524 [hep-ex]].

[3] CKMfitter Group, J. Charles *et al.*, CP violation and the CKM matrix: Assessing the impact of the asymmetric B factories, Eur. Phys. J. C **41** (2005) no.1, 1-131 [arXiv:hep-ph/0406184 [hep-ph]].

[4] UTfit Collaboration, M. Bona *et al.*, The Unitarity Triangle Fit in the Standard Model and Hadronic Parameters from Lattice QCD: A Reappraisal after the Measurements of Δm_s and $\mathcal{B}(B \to \tau\nu_\tau)$, JHEP **10** (2006), 081 [arXiv:hep-ph/0606167 [hep-ph]].

[5] LHCb Collaboration, R. Aaij *et al.*, Measurement of CP observables in the process $B^0 \to DK^{*0}$ with two- and four-body D decays, JHEP **1908** (2019) 041 [arXiv:1906.08297 [hep-ex]].

[6] LHCb Collaboration, R. Aaij *et al.*, Updated measurement of time-dependent CP-violating observables in $B_s^0 \to J/\psi K^+K^-$ decays, Eur. Phys. J. C **79** (2019) no.8, 706, Erratum: [Eur. Phys. J. C **80** (2020) no.7, 601] [arXiv:1906.08356 [hep-ex]].

[7] ATLAS Collaboration, G. Aad *et al.*, Measurement of the CP-violating phase ϕ_s in $B_s^0 \to J/\psi\phi$ decays in ATLAS at 13 TeV, [arXiv:2001.07115 [hep-ex]].

[8] CMS Collaboration, A. M. Sirunyan *et al.*, Measurement of the CP-violating phase ϕ_s in the $\mathrm{B_s^0} \to \mathrm{J}/\psi\,\phi(1020) \to \mu^+\mu^-\mathrm{K^+K^-}$ channel in proton-proton collisions at $\sqrt{s}$ = 13 TeV, [arXiv:2007.02434 [hep-ex]].

[9] LHCb Collaboration, R. Aaij *et al.*, Measurement of CP violation in $B^0 \to D^{*\pm}D^{\mp}$ decays, JHEP **2003** (2020) 147 [arXiv:1912.03723 [hep-ex]].

[10] M. Pivk and F. R. Le Diberder, SPlot: A Statistical tool to unfold data distributions, Nucl. Instrum. Meth. A **555** (2005), 356-369 [arXiv:physics/0402083 [physics.data-an]].

[11] LHCb Collaboration, R. Aaij *et al.*, Measurement of matter-antimatter differences in beauty baryon decays, Nature Phys. **13** (2017), 391-396 [arXiv:1609.05216 [hep-ex]].

[12] LHCb Collaboration, R. Aaij *et al.*, Search for CP violation and observation of P violation in $\Lambda_b^0 \to p\pi^-\pi^+\pi^-$ decays, Phys. Rev. D **102** (2020) no.5, 051101 [arXiv:1912.10741 [hep-ex]].

[13] LHCb Collaboration, R. Aaij *et al.*, Measurements of CP violation in the three-body phase space of charmless $B^\pm$ decays, Phys. Rev. D **90** (2014) no.11, 112004 [arXiv:1408.5373 [hep-ex]].

[14] LHCb Collaboration, R. Aaij *et al.*, Observation of Several Sources of CP Violation in $B^+ \to \pi^+\pi^+\pi^-$ Decays," Phys. Rev. Lett. **124** (2020) no.3, 031801 [arXiv:1909.05211 [hep-ex]].

[15] LHCb Collaboration, R. Aaij *et al.*, Amplitude analysis of the $B^+ \to \pi^+\pi^+\pi^-$ decay, Phys. Rev. D **101** (2020) no.1, 012006 [arXiv:1909.05212 [hep-ex]].